Circulation
JOURNAL OF THE AMERICAN HEART ASSOCIATION

Optical Coherence Tomographic Analysis of In-Stent Neoatherosclerosis After Drug Eluting Stent Implantation

Soo-Jin Kang, Gary S. Mintz, Takashi Akasaka, Duk-Woo Park, Jong-Young Lee, Won-Jang Kim, Seung-Whan Lee, Young-Hak Kim, Cheol Whan Lee, Seong-Wook Park and Seung-Jung Park

Circulation 2011;123;2954-2963; originally published online Jun 6, 2011;
DOI: 10.1161/CIRCULATIONAHA.110.988436
Circulation is published by the American Heart Association. 7272 Greenville Avenue, Dallas, TX 72514
 Print ISSN: 0009-7322. Online ISSN: 1524-4539

Optical Coherence Tomographic Analysis of In-Stent Neoatherosclerosis After Drug–Eluting Stent Implantation

Soo-Jin Kang, MD; Gary S. Mintz, MD; Takashi Akasaka, MD, PhD; Duk-Woo Park, MD, PhD; Jong-Young Lee, MD; Won-Jang Kim, MD; Seung-Whan Lee, MD, PhD; Young-Hak Kim, MD, PhD; Cheol Whan Lee, MD, PhD; Seong-Wook Park, MD, PhD; Seung-Jung Park, MD, PhD

Background—We report findings from optical coherence tomography (OCT) of in-stent neoatherosclerosis as a cause of drug-eluting stent (DES) failure.

Methods and Results—Optical coherence tomography and grayscale and virtual histology intravascular ultrasound were performed in 50 patients (30 stable, 20 unstable angina) with 50 DES in-stent restenosis lesions and intimal hyperplasia >50% of stent area. Median follow-up time was 32.2 months. Overall, 26 lesions (52%) had at least 1 OCT-defined in-stent thin-cap fibroatheroma (TCFA)–containing neointima and 29 (58%) had at least 1 in-stent neointimal rupture. Patients presenting with unstable angina showed a thinner fibrous cap (55 μm [interquartile range 42 to 105 μm] versus 100 μm [interquartile range 60 to 205 μm], $P=0.006$) and higher incidence of OCT-defined TCFA-containing neointima (75% versus 37%, $P=0.008$), intimal rupture (75% versus 47%, $P=0.044$), thrombi (80% versus 43%, $P=0.010$), and red thrombi (30% versus 3%, $P=0.012$) than stable patients. Fibrous cap thickness negatively correlated with follow-up time ($r=-0.318$, $P=0.024$). Compared with DES <20 months after implantation (the best cut-off to predict TCFA-containing neointima), DES ≥20 months after implantation had a higher incidence of TCFA-containing neointima (69% versus 33%, $P=0.012$) and red thrombi (27% versus 0%, $P=0.007$). Patients with unstable (versus stable) angina had an increasing number of unstable OCT findings including TCFA-containing neointima, neointima rupture, and thrombus ($P=0.027$). The rate of agreement between grayscale intravascular ultrasound and OCT for detecting intimal rupture was 50% and for detecting thrombus was 44%. The agreement between virtual histology intravascular ultrasound and OCT for identifying TCFA-containing neointima was 78%.

Conclusions—In-stent neoatherosclerosis may be an important mechanism of DES failure, especially late after implantation. **(*Circulation*. 2011;123:2954-2963.)**

Key Words: optical coherence tomography ■ vascular graft restenosis ■ atherosclerosis

In-stent restenosis (ISR) is generally considered to be a stable process, with an early peak in intimal hyperplasia (IH) followed by a quiescent period beginning 1 year after stent implantation.[1–3] However, recent studies have reported that one third of patients with ISR present with acute coronary syndromes.[4,5] Furthermore, there is emerging histological and angioscopic evidence of late de novo in-stent neoatherosclerosis.[6–10] Using virtual histology intravascular ultrasound (VH-IVUS) analysis we recently reported that in-stent percentage necrotic core (%NC) and percentage dense calcium (%DC) increase over time in both bare metal stent and drug-eluting stent (DES)–treated lesions.[11] Most recently, an optical coherence tomography (OCT) study demonstrated that neointima within bare metal stent may transform into lipid-laden atherosclerotic plaque.[12] These studies indicate (1) that in some patients there is degenerative evolution of neointima into an unstable atherosclerotic lesion and (2) that ISR should not always be regarded as a benign entity. The aims of the current study were to report the OCT spectrum of in-stent neoatherosclerosis within DES-treated lesions that presented with ISR and to compare the OCT and grayscale and VH-IVUS findings of in-stent neointimal hyperplasia and in-stent neoatherosclerosis.

Editorial see p 2913
Clinical Perspective on p 2963

Methods

Subjects

From February 2007 to November 2010, OCT was performed on 54 consecutive patients with DES restenosis (diameter stenosis >50% by visual estimation at follow-up angiography). Exclusion criteria

Received September 14, 2010; accepted March 23, 2011.

From the Department of Cardiology, University of Ulsan College of Medicine, Asan Medical Center, Seoul, Korea (S.K., D.P., J.L., W.K., S.L., Y.K., C.W.L., S.-W.P., S.-J.P.); Cardiovascular Research Foundation, New York, NY (G.S.M.); and the Division of Cardiovascular Medicine, Wakayama Medical University, Japan (T.A.).

The online-only Data Supplement is available with this article at http://circ.ahajournals.org/cgi/content/full/CIRCULATIONAHA.110.988436/DC1.

Correspondence to Seung-Jung Park, MD, PhD, Professor of Medicine, Asan Medical Center, 388-1 Poongnap-dong, Songpa-gu, Seoul, South Korea, 138-736. E-mail sjpark@amc.seoul.kr

Circulation **is available at http://circ.ahajournals.org** **DOI: 10.1161/CIRCULATIONAHA.110.988436**

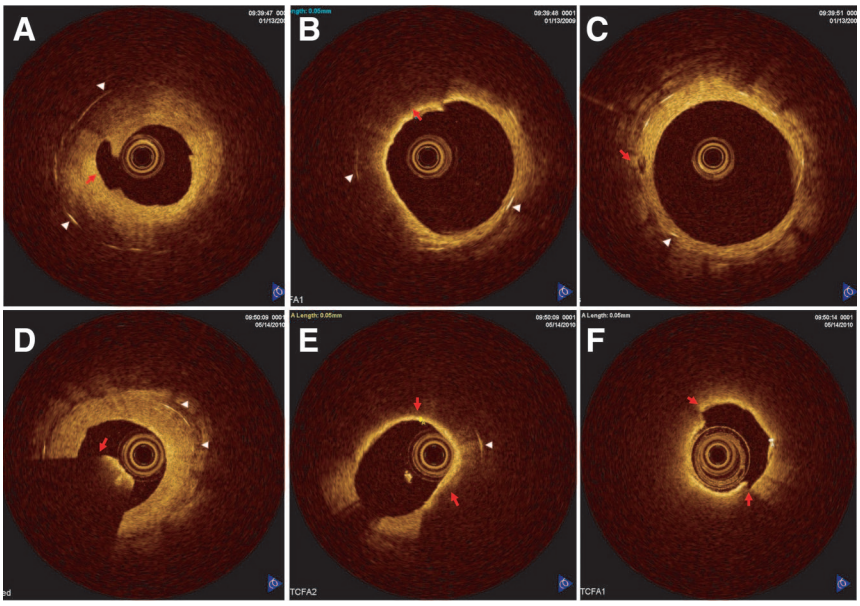

Figure 1. Optical coherence tomography findings of neointima inside DES. All white arrows indicate stent struts. **A** through **C**, A 71-year-old woman who underwent DES implantation at mid-RCA 65 months previously presented with stable angina. **A**, Intimal rupture (red arrow); **B**, TCFA-containing neointima surrounded by signal-poor lipidic area (red arrow); **C**, fibrotic neointima with microvessels (red arrow). **D** through **F**, A 70 year-old man who underwent DES implantation at mid–left anterior descending artery 60 months previously presented with unstable angina. **D**, Intraluminal red thrombus with fast attenuation (red arrow); **E**, TCFA-containing neointima (red arrow) with lipidic tissue; **F**, intimal rupture (red arrow) surrounded by TCFA-containing neointima. The minimal thickness of fibrous cap was measured at 60 μm. TCFA indicates thin-cap fibroatheroma.

were hemodynamic instability, an inability of the OCT imageWire to cross the ISR lesion into the distal vessel because of tight stenosis or severe vessel tortuosity, left main or saphenous vein graft lesions, myocardial infarction, or the presence of angiographically visible thrombus. Optical coherence tomography image analysis was performed at the Asan Medical Center, Seoul, Korea. Because the purpose of study was to characterize neointimal tissue in DES-treated lesions, 1 patient with thrombotic coronary occlusion without significant neointima and 3 ISR patients with dominant-stent underexpansion and little neointima were excluded from the analysis. Finally, 50 patients (30 stable angina and 20 unstable angina) were included in the current study. Virtual histology IVUS were performed in 32 of 50 patients (20 stable and 12 unstable angina) in whom IVUS catheters could cross the ISR lesions after OCT imaging. All patients signed written informed consent before being enrolled in the study.

Angiographic Analysis

Qualitative and quantitative angiographic measurements were performed using standard techniques with automated edge-detection algorithms (CASS-5, Pie-Medical, the Netherlands) in the angiographic analysis center of the Cardiovascular Research Foundation, Seoul, Korea.[13–16] Angiographic restenosis was defined as a diameter stenosis >50% at follow-up angiography and classified as suggested by Mehran et al.[13]

Optical Coherence Tomography Imaging and Analysis

The time-domain OCT procedure using the occlusive technique and its anatomic limitations have been previously reported.[17] Optical coherence tomography image acquisition was performed using a commercially available system for intracoronary imaging and a 0.019-inch ImageWire (LightLab Imaging, Westford, MA) before IVUS imaging. The artery was cleared from blood by applying continuous flush delivery as described previously.[18] Flush consisted of iodixanol 370 (Visipaque, GE Health Care, Cork, Ireland) at a flow rate of 3.0 mL/s.

Neointima was the tissue between the luminal border and the inner border of the struts. Intimal hyperplasia area was calculated as stent minus intrastent lumen; and % IH was calculated as IH area divided by stent area. Calcific intima was defined as a well-delineated, signal-poor region with sharp borders. Lipidic intima was defined as a signal-poor region with diffuse borders.[19]

Thin-cap fibroatheroma (TCFA)–containing intima was defined as fibrous cap thickness at the thinnest part ≤65 μm and an angle of lipidic tissue ≥180°.[20] Multiple OCT-defined TCFA-containing neointima were separated by at least 3 mm. Optical coherence tomography neointimal rupture was a break in the fibrous cap that connected the lumen with the underlying lipid pool.[21] Thrombi were masses protruding into the vessel lumen, discontinuous from the surface of the vessel wall and with a dimension ≥250 μm. Red thrombi were characterized as high-backscattering protrusions with signal-free shadowing. White thrombi were characterized by signal-rich low-backscattering projections into the lumen.[12,21–23] When attenuation caused by large amounts of red thrombus obscured underlying neointima morphology, OCT-detectable TCFA-containing neointima and neointima rupture were identified proximal or distal (or opposite) to the red thrombus.

The axial location of the TCFA-containing intima and/or intimal rupture was assessed (1) at the minimal lumen area site (within 5 mm from the minimal lumen area frame), (2) proximal to the minimal lumen area site, or (3) distal to the minimal lumen area site. The maximal area of each thrombus was measured, and the length of the in-stent segment involved with thrombi was semiquantified as <25%, 25% to 75%, or >75% of total stent length.

A microvessel (evidence of neovascularization) was defined as a small vesicular or tubular structure with a diameter ≤200 μm.[24] Intraintimal neovascularization was located within the most superficial 50% of the neointimal thickness, and peristent neovascularization was located within the deepest 50% of the neointimal thickness.[12] Stent strut coverage was assessed as previously described.[23]

All reported OCT parameters required the agreement of 3 observers (S.J.K., G.S.M., and T.A.) who were blinded to the clinical and procedural characteristics. Examples are shown in Figure 1.

Intravascular Ultrasound Imaging and Analysis

Intravascular ultrasound imaging was performed after OCT image acquisition and after intracoronary administration of 0.2 mg nitroglycerin using motorized transducer pullback (0.5 mm/s) and a commercial scanner (Boston Scientific/SCIMED, Minneapolis, MN) consisting of a rotating 40MHz transducer within a 3.2Fr imaging sheath. Quantitative volumetric IVUS analysis was performed as previously described.[25,26] Using computerized planimetry (EchoPlaque 3.0, Indec Systems, Mountain View, CA), stent and reference segments were assessed. Measurements included external elastic membrane (EEM), stent, lumen (intrastent lumen bounded by the borders of the stent and/or IH), and IH (IH =stent minus intrastent lumen) areas. Percentage IH was defined as IH area divided by stent area. Stent underexpansion was defined as minimal stent area <5 mm^2.[27,28] Significant IH was defined as % IH area >50%.

Table 1. Baseline Clinical and Procedural Characteristics

Variable	Total	Stable	Unstable	P*
N	50	30	20	
Baseline clinical characteristics				
Age, y	64.5 (54.0 to 68.3)	64.0 (54.0 to 68.0)	65.5 (54.0 to 69.8)	0.475
Male, n (%)	39 (78)	25 (83)	14 (70)	0.221
Smoking, n (%)	24 (48)	15 (50)	9 (45)	0.477
Hypertension, n (%)	28 (56)	20 (67)	8 (40)	0.063
Hypercholesterolemia, n (%)	42 (84)	26 (87)	16 (80)	0.529
Diabetes mellitus, n (%)	17 (34)	7 (23)	10 (50)	0.051
Statin therapy, n (%)	25 (50)	17 (57)	8 (40)	0.584
Left ventricular ejection fraction, %	60.0 (55.0–62.0)	60.0 (59.3 to 63.8)	57.5 (50.0 to 60.8)	0.078
Previous coronary bypass surgery, n (%)	2 (4)	2 (7)	0 (0)	0.239
Previous myocardial infarction, n (%)	5 (10)	3 (10)	2 (10)	1.000
Pre-PCI peak troponin I (ng/mL)‡			0.02 (0.01–0.15)	
Baseline CK-MB (ng/mL)†	1.0 (0.6 to 1.7)	0.7 (0.6 to 1.2)	1.6 (0.5 to 2.0)	0.149
Pre-PCI peak CK-MB (ng/mL)†	1.0 (0.6 to 2.0)	0.8 (0.6 to 1.4)	1.7 (0.4 to 2.5)	0.177
Post-PCI peak CK-MB (ng/mL)†	1.4 (0.9 to 2.1)	1.2 (0.8 to 2.1)	1.7 (0.9 to 4.6)	0.365
Types of drug-eluting stent				0.203
Cypher, n (%)	25 (50)	12 (40)	13 (65)	
Taxus, n (%)	10 (20)	9 (30)	1 (5)	
Endeavor, n (%)	3 (6)	2 (7)	1 (5)	
Xience, n (%)	2 (4)	1 (3)	1 (5)	
Other drug-eluting stent, n (%)	10 (20)	6 (20)	4 (20)	
Total stent length, mm	31.9 (23.3 to 49.8)	30.1 (23.1 to 51.2)	33.8 (26.9 to 49.3)	0.802

Values are median (IQR) unless otherwise specified. PCI indicates percutaneous coronary intervention; CK-MB, creatine kinase MB.
*P: stable angina vs unstable angina.
†Normal reference value of CK-MB: 0 to 5.0 ng/mL.
‡Normal reference value of troponin I: 0 to 1.5 ng/ml. Troponin I was measured in 12 patients with unstable angina.

Intravascular ultrasound neointimal rupture was identified by the presence of an intra-IH cavity that communicated with the lumen with an overlying residual fibrous cap fragment.

Virtual Histology Intravascular Ultrasound Analysis

Virtual histology IVUS was performed after OCT and grayscale IVUS studies after intracoronary administration of 0.2 mg nitroglycerin using the 2.9Fr Eagle Eye, (Volcano Corp, Rancho Cordova, CA) IVUS catheter that incorporated a 20-MHz electronic-array transducer. The transducer was advanced into the distal reference segment, and an imaging run was performed back through the stent to the proximal reference segments using the R-100 motorized transducer pullback device (0.5 mm/s). By use of pcVH software (Volcano Corp), the region of interest was placed between the luminal border and the inner border of the struts to avoid stent strut artifacts. Virtual histology IVUS analysis coded tissue as green (fibrotic), yellow-green (fibrofatty), white (DC), and red (NC).[29,30] Neointima tissue component was represented as percentages of measured IH (%fibrous, %fibrofatty, %NC, and %DC). In parallel with the criteria of native VH-TCFA, a VH-defined TCFA-containing neointima was a lesion fulfilling the following criteria: confluent NC >10% of in-stent neointima and no evidence of an overlying fibrous cap in at least 3 frames, as previously described by Rodriguez-Granillo et al.[30] Multiple VH-defined TCFA-containing neointima were considered if they were separated by ≥3 consecutive non-TCFA–containing image slices.

Statistical Analysis

All statistical analyses were performed using SPSS (version 10.0, SPSS Inc, Chicago, IL). All values are expressed as the median (interquartile range [IQR]) or as counts and percentages (categorical variables). Continuous variables were compared by use of the nonparametric Mann–Whitney test; categorical variables were compared with χ^2 statistics or the Fisher exact test. Receiver operating curve was analyzed to assess the best cut-off values of follow-up time predicting TCFA-containing intima with a maximal accuracy using MedCalc (MedCalc Software, Mariakerke, Belgium). A P value <0.05 was considered statistically significant.

Results

Baseline Clinical and Procedural Characteristics

The clinical and procedural characteristics of the 50 ISR patients are summarized in Table 1. The median follow-up time was 32.2 months (IQR 9.2 to 52.3). At the time of follow-up angiography, 30 patients (60%) presented with stable angina and 20 (40%) with unstable angina. Overall, 27 ISR lesions had 1 DES, 19 ISR lesions had 2 overlapping DES, and 4 ISR lesions had 3 overlapping DES.

Angiographic and Intravascular Ultrasound Findings

Quantitative angiographic and grayscale IVUS data are presented in Table 2. At the minimal lumen area (MLA) site using IVUS, 8 stents (16%) were underexpanded. Also using IVUS, in-stent neointimal rupture was detected in 10 lesions (20%), and thrombi were detected in 8 lesions (16%).

Table 2. Angiographic and IVUS Data

Variable	Total	Stable	Unstable	P*
N	50	30	20	
Angiographic findings				
Lesion location, n (%)				0.825
Left anterior descending	31 (62)	19 (63)	12 (60)	
Left circumflex	2 (4)	1 (3)	1 (5)	
Right coronary	17 (34)	10 (33)	7 (35)	
Proximal reference diameter, mm	3.3 (3.0 to 3.6)	3.2 (2.9 to 3.5)	3.4 (3.2 to 3.7)	0.396
Distal reference diameter, mm	2.6 (2.2 to 3.0)	2.6 (2.2 to 2.8)	2.9 (2.1 to 3.0)	0.434
Minimal lumen diameter, mm	0.9 (0.5 to 1.1)	1.0 (0.7 to 1.3)	0.6 (0.3 to 1.0)	0.010
Diameter stenosis,%	69.0 (58.3 to 83.5)	63.0 (50.0 to 74.5)	82.0 (65.0 to 88.0)	0.002
TIMI flow, n (%)				0.888
TIMI 0	4 (8)	2 (7)	2 (10)	
TIMI 1	2 (4)	1 (3)	1 (5)	
TIMI 2	7 (14)	5 (17)	2 (10)	
TIMI 3	37 (74)	22 (73)	15 (75)	
Stent fracture, n (%)	4 (8)	4 (13)	0 (0)	0.188
Mehran Classification, n (%)				0.583
Focal in-stent restenosis	28 (56)	17 (57)	11 (55)	
Multifocal in-stent restenosis	3 (6)	2 (7)	1 (5)	
Diffuse in-stent restenosis	17 (34)	11 (36)	6 (30)	
Total in-stent restenosis	2 (4)	0 (0)	2 (10)	
IVUS findings				
Proximal reference lumen area, mm^2	7.1 (5.5 to 9.1)	6.8 (5.3 to 8.2)	7.8 (6.4 to 9.4)	0.394
Proximal reference EEM area, mm^2	15.5 (11.8 to 17.7)	15.3 (11.7 to 17.8)	16.2 (11.9 to 17.9)	0.637
Distal reference lumen area, mm^2	4.6 (3.6 to 6.1)	4.4 (3.2 to 5.8)	4.9 (3.7 to 6.6)	0.567
Distal reference EEM area, mm^2	8.1 (6.4 to 11.1)	7.6 (6.0 to 11.0)	8.6 (6.9 to 11.9)	0.551
Minimal stent area, mm^2	5.7 (4.6 to 7.4)	5.5 (4.4 to 7.4)	5.8 (4.9 to 7.7)	0.445
Minimal lumen area, mm^2	1.8 (1.2 to 2.5)	1.8 (1.2 to 2.4)	1.8 (1.4 to 2.5)	0.301
Stent area at the minimal lumen site, mm^2	7.0 (5.3 to 8.5)	7.3 (5.4 to 8.5)	6.9 (5.2 to 8.5)	0.934
IH, %	71.8 (64.4 to 80.5)	75.1 (66.3 to 81.6)	70.5 (57.8 to 78.1)	0.210
Underexpansion (minimal stent area <5.0 mm^2), n (%)	14 (28)	8 (27)	6 (30)	0.629

IVUS indicates intravascular ultrasound; TIMI, Thrombolysis In Myocardial Infarction; EEM, external elastic membrane; and IH, intimal hyperplasia.

Values are median (IQR) unless otherwise specified.

*P: stable angina vs unstable angina.

Overall Optical Coherence Tomography Findings

Overall, 26 lesions (52%) had at least 1 site of in-stent TCFA-containing neointima; and 29 (58%) had at least 1 site of in-stent neointimal rupture. Among lesions with OCT-identified neointimal rupture, 10 (34%) showed IVUS-defined neointimal rupture; conversely, all lesions with IVUS-defined neointimal rupture showed OCT-defined neointimal rupture. The axial distribution of the neointimal ruptures was at the MLA site in 49%, proximal to the MLA site in 36%, and distal to the MLA site in 15%. In addition, the axial distribution of the TCFA- containing neointima was at the MLA site in 56%, proximal to the MLA site in 28%, and distal to the MLA site in 16%. Lesions with focal ISR (by Mehran classification) were less frequently associated with OCT-defined TCFA-containing neointima compared with multifocal, diffuse, and total occlusion ISR (39% versus 68%, $P=0.040$). In 4 lesions with angiographic stent fracture, only 1 lesion showed all 3 OCT findings (intimal rupture, TCFA-containing neointima, and thrombi) whereas the remaining 3 lesions had none of these findings.

Optical Coherence Tomography Findings According to Clinical Presentation

In Table 3, OCT characteristics are compared in patients with unstable angina versus stable angina. Overall, 90% of lesions had in-stent lipid-containing neointima. Compared with the stable angina group, the unstable angina group had a thinner fibrous cap ($P=0.006$) and a higher incidence of TCFA-containing neointima ($P=0.008$) and intimal rupture ($P=0.044$). The number of neoatherosclerotic OCT findings was greater in patients with an unstable angina presentation than in those with a stable presentation ($P=0.027$).

Table 3. OCT Findings According to Clinical Presentation

		Clinical Presentation		
	Total	Stable	Unstable	*P*
N	50	30	20	
Follow-up duration, mo	32.2 (9.2 to 52.2)	14.2 (8.1 to 51.7)	40.6 (16.6 to 56.9)	0.178
Lipid neointima, n (%)	45 (90)	25 (83)	20 (100)	0.067
Calcium, n (%)	5 (10)	2 (7)	3 (15)	0.310
Minimal thickness of fibrous cap, μm	60 (50 to 162)	100 (60 to 205)	55 (42 to 105)	0.006
Incidence of thrombi, n (%)	29 (58)	13 (43)	16 (80)	0.010
Incidence of red thrombi, n (%)	7 (14)	1 (3)	6 (30)	0.012
Maximal area of thrombi, mm^2	0.6 (0.3 to 1.3)	0.4 (0.3 to 0.9)	1.0 (0.4 to 1.5)	0.092
Incidence of intimal rupture, n (%)	29 (58)	14 (47)	15 (75)	0.044
Incidence of multiple ruptures, n (%)	8 (16)	4 (13)	4 (20)	0.095
Incidence of TCFA, n (%)	26 (52)	11 (37)	15 (75)	0.008
Incidence of multiple TCFA, n (%)	6 (12)	2 (7)	4 (20)	0.626
Neovascularization, n (%)	30 (60)	15 (50)	15 (75)	0.069
None of 3 major findings	13 (26)	12 (40)	1 (5)	0.027*
One finding, n (%)	8 (16)	5 (17)	3 (15)	
TCFA only, n (%)	2 (4)	2 (7)	0 (0)	
Rupture only, n (%)	2 (4)	1 (3)	1 (5)	
Thrombi only, n (%)	4 (8)	2 (7)	2 (10)	
Two findings, n (%)	11 (22)	6 (20)	5 (25)	
TCFA+rupture, n (%)	4 (8)	2 (7)	2 (10)	
TCFA+thrombi, n (%)	2 (4)	0 (0)	2 (10)	
Rupture+thrombi, n (%)	5 (10)	4 (13)	1 (5)	
All 3 findings (TCFA+rupture+thrombi), n (%)	18 (36)	7 (23)	11 (55)	
Stent coverage				0.920
Embedded, n (%)	29 (58)	17 (57)	12 (60)	
Protruded, covered, n (%)	8 (16)	5 (17)	3 (15)	
Protruded, uncovered, n (%)	9 (18)	5 (17)	4 (20)	
Malapposed, n (%)	4 (8)	3 (10)	1 (5)	

Continuous variables are presented as median (IQR) and compared using nonparametric Mann–Whitney test.
*Comparing no findings vs 1 finding vs 2 findings vs 3 findings.

Thrombi were identified in 29 patients (58%). The length of thrombi was shorter than 25% of total stent length in 25 of the thrombi-containing lesions (86%). Thrombi were more common in patients with unstable angina (80% versus 43%, $P=0.010$) than in those with stable angina. In addition, red thrombi were also more common in patients with unstable angina (30% versus 3%, $P=0.012$).

Optical Coherence Tomography Findings According to Follow-Up Duration

Overall, the 26 lesions with a TCFA-containing neointima presented later than the 24 lesions without a TCFA-containing neointima: 42.3 months (IQR 16.0 to 63.0) versus 11.6 months (IQR 8.0 to 47.4) ($P=0.020$). Using receiver-operating curve analysis, 20 months was the best predictor of the presence of a TCFA-containing neointima with a sensitivity of 73% and a specificity of 67% (area under curve =0.692, 95% confidence interval =0.546 to 0.815, $P=0.001$). In Table 4, OCT characteristics are analyzed using this cut-off value. Comparing ISR patients who presented within 20 months post-stent implantation to those who presented after 20 months, the fibrous cap was thinner, and the incidence of TCFA-containing neointima and multiple TCFA-containing neointima was greater, but the frequency of intimal ruptures and thrombi was similar. There was also a trend that unstable angina presentation was more frequent in patients who presented after 20 months compared to patients who presented within 20 months post-stent implantation (50% versus 29%, $P=0.112$).

In Figure 2, we compared patients who presented <12 months, 12 to 36 months, and >36 months after stent implantation. Thin-cap fibroatheroma–containing neointima (29% versus 50% versus 68%, $P=0.016$) and multiple TCFA-containing neointima (0% versus 0% versus 24%, $P=0.012$) were more common in patients who presented after 36 months than in those who presented earlier. Although the incidence of thrombi was not different among the 3 groups (53% versus 50% versus 64%, $P=0.684$), red thrombi (0%

Table 4. OCT Findings According to Follow-Up Time

	Follow-Up <20 mo	Follow-Up ≥20 mo	*P*
N	24	26	
Lipid neointima, n (%)	21 (88)	24 (92)	0.461
Calcium, n (%)	1 (4)	4 (15)	0.200
Minimal thickness of fibrous cap, μm	100 (60 to 220)	60 (50 to 122.5)	0.020
Incidence of thrombi, n (%)	13 (54)	16 (62)	0.405
Incidence of red thrombi, n (%)	0 (0)	7 (27)	0.007
Maximal area of thrombi, mm^2	0.4 (0.3 to 0.8)	1.1 (0.5 to 1.5)	0.015
Incidence of intimal rupture, n (%)	13 (54)	16 (62)	0.405
Incidence of multiple ruptures, n (%)	3 (13)	5 (19)	0.399
Incidence of TCFA, n (%)	8 (33)	18 (69)	0.012
Incidence of multiple TCFA, n (%)	0 (0)	6 (23)	0.014
Neovascularization, n (%)	13 (54)	17 (65)	0.302
None of 3 major findings	8 (33)	5 (19)	0.073*
One finding, n (%)	3 (13)	5 (19)	
TCFA only	0 (0)	2 (8)	
Rupture only	1 (4)	1 (4)	
Thrombi only	2 (8)	2 (8)	
Two findings, N (%)	8 (33)	3 (12)	
TCFA+rupture	2 (8)	2 (8)	
TCFA+thrombi	1 (4)	1 (4)	
Rupture+thrombi	5 (21)	0 (0)	
All 3 findings (TCFA+rupture+thrombi), n (%)	5 (21)	13 (50)	
Stent coverage, n (%)			0.667
Embedded	14 (58)	15 (58)	
Protruded, covered	5 (21)	3 (12)	
Protruded, uncovered	4 (17)	5 (19)	
Malapposed	1 (4)	3 (12)	

Continuous variables are presented as median (IQR) and compared using nonparametric Mann–Whitney test.

*Comparing no findings vs 1 finding vs 2 findings vs 3 findings.

versus 0% versus 28%, $P=0.017$) were more frequent in patients who presented after 24 months than in those who presented earlier. Finally, OCT-measured fibrous cap thickness negatively correlated with time to presentation ($r=-0.318$, $P=0.024$).

Virtual Histology Intravascular Ultrasound Findings

The median follow-up time in 32 patients (20 stable and 12 unstable angina) who also had VH-IVUS imaging was 17.2 months (IQR 8.9 to 50.8). Overall, 13 ISR lesions (41%) showed NC >10% at the MLA site, and 24 (75%) had NC >10% at the maximal NC site. Compared to lesions with ≤10% NC at the MLA site, lesions with >10% NC had significantly longer time to ISR presentation (46.3 months [IQR 14.7 to 63.3] versus 10.2 months [IQR 7.7 to 43.7], $P=0.040$). Figure 3 shows the frequency of VH-defined TCFA-containing neointima according to follow-up duration.

Virtual histology–defined TCFA-containing neointima was seen in 10 lesions (31%). The 10 lesions with a TCFA-containing neointima presented later than the 22 lesions without a TCFA-containing neointima: 49.2 months (IQR 15.9 to 66.8) versus 11.6 months (IQR 7.7 to 41.6), ($P=0.006$). Also, there was a positive correlation between follow-up time and %DC at the maximal %NC site ($r=0.510$, $P=0.015$).

Comparison Among Optical Coherence Tomography, Grayscale, and Virtual Histology Intravascular Ultrasound Findings

The clinical and procedural characteristics of the 32 DES-ISR patients who had imaging using all 3 modalities (grayscale, VH-IVUS, and OCT) are described in online-only Data Supplement Table I. The angiographic, IVUS, VH-IVUS, and OCT findings are summarized in the online-only Data Supplement Tables II through IV. Table 5 compares (1) identification of neointimal rupture by both grayscale IVUS and OCT, (2) identification of TCFA-containing neointima by both VH and OCT, and (3) detection of thrombi by both grayscale IVUS and OCT in the subgroup of patients who had imaging using all 3 modalities. The rate of agreement between grayscale IVUS and OCT for detecting intimal rupture was 50% and for detecting thrombus was 44%. The agreement between VH-IVUS and OCT for identifying TCFA-containing neointima was 78%. Using OCT as the gold standard, the sensitivity and specificity of VH-defined TCFA-containing neointima was 60% and 94%, respectively, with positive and negative predictive values of 90% and 73%, respectively.

The 22 lesions with OCT-defined TCFA-containing neointima had larger %NC at the MLA site compared with 18 lesions without an OCT-defined TCFA-containing neointima (25.2% [IQR 8.6 to 30.0] versus 4.7% [IQR 1.3 to 11.4], $P=0.001$). This was also true at the maximal NC site for %NC (33.2% [IQR 27.5 to 42.5] versus 12.8% [IQR 6.0 to 24.2], $P<0.001$) and for %DC (5.5% [IQR 2.4 to 8.5] versus 0.6% [IQR 0.0 to 1.7], $P<0.001$). Conversely, lesions with VH-defined TCFA-containing neointima had a much thinner fibrous cap measured by OCT than lesions without a VH-defined TCFA-containing neointima (50.0 μm [IQR 40.0 to 52.5] versus 120.0 μm [60.0 to 220.0], $P=0.001$).

Revascularization

All but 1 patient underwent target lesion revascularization (repeat percutaneous coronary intervention [PCI] in 48 patients and coronary artery bypass surgery in 2 patients). Pre-PCI Thrombolysis In Myocardial Infarction (TIMI) 3 flow was observed in 37 lesions (78%). Compared with lesions with TIMI 3 flow, the 13 lesions with TIMI <3 flow more frequently showed TCFA-containing neointima (85% versus 41%, $P=0.007$) and intimal rupture (85% versus 48%, $P=0.024$). In addition, the fibrous cap was thicker in the lesions with TIMI <3 flow (50 μm [IQR 50 to 60] versus 90 μm [IQR 60 to 190], $P=0.016$). The peak post-PCI creatine-kinase MB (CK-MB) showed subtle but significant

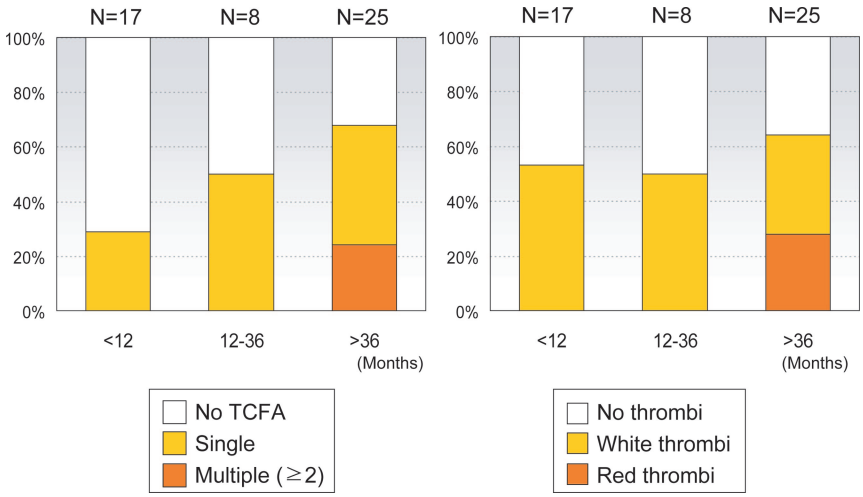

Figure 2. Frequency of OCT-defined TCFA-containing neointima (single and multiple) and thrombi (white and red) in 50 ISR lesions with DES implantation according to follow-up time. TCFA indicates thin-cap fibroatheroma.

elevation in patients showing intimal rupture versus no intimal rupture (1.8 ng/mL [IQR 1.0 to 5.9] versus 1.1 ng/mL [IQR 0.7 to 1.6], $P=0.025$).

Discussion

In the current study, OCT findings indicating in-stent neoatherosclerosis were frequently identified in patients with DES-ISR, especially late DES-ISR, including TCFA-containing intima in 52%, intimal rupture in 58%, and thrombi in 58%. Irrespective of clinical presentations of DES-ISR (unstable or stable angina), 90% of the lesions had lipid-containing neointima. Even in stable angina patients, one third showed TCFA-containing intima and half had in-stent intimal rupture. Neointimal fibrous cap thickness decreased over time, with a follow-up duration >20 months being the best cut-off value to predict the presence of TCFA-containing intima. All of these findings suggest either atherosclerotic neointimal degenerative changes over time or neoatherosclerosis superimposed on a stable neointimal platform, consistent with our recent data using VH-IVUS analysis.[11] Furthermore, VH subgroup analysis in the current study supported OCT findings in that the presence of VH-defined TCFA-containing neointima and high content of NC was related to the longer follow-up duration.

Although Gonzalo et al previously reported various OCT patterns of restenotic tissue after stenting (84% were various DES), the median follow-up time was only 12 months, too short to manifest the entire spectrum of neoatherosclerosis as suggested in the current study; in the current study, the best predictor of a TCFA-containing neointima was a 20-month follow-up period after DES implantation.[24] Furthermore, the current study showed that patients with late DES-ISR were more likely to have an unstable clinical presentation compared to those with early DES-ISR.

Recently, Takano et al suggested that lipid-laden neointima, neointimal disruption, and thrombus as detected by OCT were more frequently found late (≥5 years) in comparison with early (<6 months) after bare metal stent implantation.[12] This was also similar to our observations in DES-treated lesions. However, our findings suggested that the transformation into atheromatous lipid-laden tissue occurred earlier after DES implantation than after bare metal stent implantation, consistent with the angioscopic findings of Higo et al[10] and the histological findings of Nakazawa et al.[31,32]

Although thrombi were observed in 43% of stable angina ISR patients, most were white thrombi that were of relatively small size. In the current study, the presence of thrombi, especially red thrombi, was associated with unstable angina.

The higher incidence of in-stent TCFA-containing neointima, thrombi, and neointimal rupture in unstable angina patients supported the concept that these OCT findings were similar to vulnerable plaque in a native coronary artery. Our previous VH-IVUS study suggested that neoatherosclerosis with a large necrotic core can develop within previously placed stents.[11] Furthermore, in the current study, TIMI flow at presentation was reduced in lesions showing neointimal rupture or TCFA-containing neointima, and preprocedural OCT findings of neointimal rupture significantly correlated

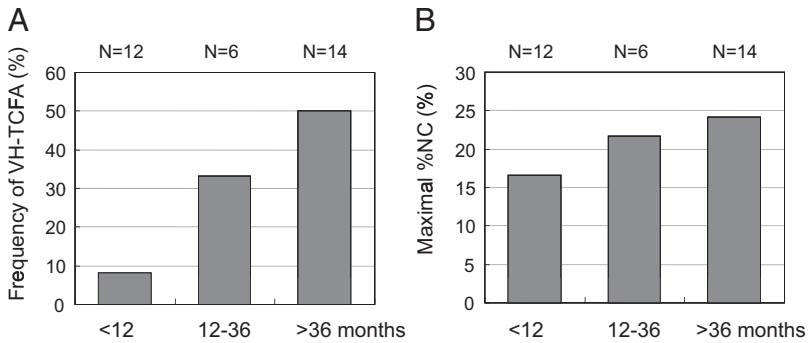

Figure 3. Frequency of VH-defined TCFA-containing neointima according to follow-up duration in 32 patients who presented <12 months (n=12), 12 to 36 months (n=6), and >36 months (n=14) after stent implantation (**A**). Maximal %NC according to the follow-up time (**B**). VH-TCFA indicates virtual histology thin-cap fibroatheroma; %NC, percentage necrotic core.

Table 5. Comparison of Identification of Intimal Rupture and TCFA-Containing Neointima in 32 Lesions With VH Data

	(+)	(−)	Total
OCT-defined intimal rupture*			
Grayscale IVUS-defined intimal rupture			
(+)	3	0	3
(−)	16	13	29
Total	19	13	32
OCT-defined TCFA†			
VH-defined TCFA			
(+)	9	1	10
(−)	6	16	22
Total	15	17	32
OCT-defined thrombi‡			
Grayscale IVUS-defined thrombi			
(+)	3	1	4
(−)	17	11	28
Total	20	12	32

TCFA indicates thin-cap fibroatheroma; OCT, optical coherence tomography; IVUS, intravascular ultrasound; and VH, virtual histology.

*Agreement=16/32 (50%).

†Agreement=25/32 (78%).

‡Agreement=14/32 (44%).

with the peak level of post-PCI CK-MB similar to percutaneous revascularization in unstable native artery lesions.

Mostly using IVUS, we previously reported in-stent neointimal rupture as a cause of very late stent thrombosis.[33] In this previous study, disease progression with in-stent neointimal rupture was observed in 43.5% of DES lesions and 100% of bare metal stent lesions, suggesting that rupture of in-stent neoatherosclerosis was an important mechanism of very late stent thrombosis. With the excellent resolution of OCT, the current study clarified that many ISR lesions developed neoatherosclerotic changes within the neointima, especially late after implantation. However, it was not clear why some in-stent neoatherosclerosis culminated in acute coronary syndrome and some did not. Furthermore, the current data did not indicate whether all DES-treated lesions would eventually develop in-stent neoatherosclerosis or only some lesions and why.

Owing to the greater spatial resolution of OCT, the incidences of OCT-detected neointimal rupture and thrombi were higher compared with grayscale IVUS. This is similar to the observations of de novo atherosclerotic plaque rupture (73% versus 40%) and thrombi (100% versus 33%) assessed by OCT versus grayscale IVUS in patients with acute myocardial infarction.[34] As in native coronary arteries, these OCT findings suggest that atherosclerotic degeneration of the neointima with development of a TCFA-containing neointima may lead to neointimal rupture and stent thrombosis, as shown previously.[33] Using OCT as the gold standard, grayscale IVUS poorly predicted OCT-defined neointimal rupture, with a sensitivity of 16%, a specificity of 100%, a positive predictive value of 100%, and negative predictive value of 45%. Additionally, grayscale IVUS predicted OCT-defined thrombi with a sensitivity of 15% and a specificity of 92%.

In the current study, the agreement of VH-IVUS and OCT-defined TCFA-containing intima was 78%. Sawada et al previously reported the discrepancy in the frequency of TCFA detected by VH-IVUS and OCT in native plaques.[35] Although OCT has the potential to visualize the thin fibrous cap and evaluate detailed structures, large calcified lesions may be misdiagnosed as TCFA because of low signal penetration of OCT. Conversely, mural thrombi or superficial dense calcium might obscure the presence of VH-defined TCFA-containing intima. Nevertheless, the OCT and VH-IVUS findings in the current analysis seemed to be linked in that VH %NC was much greater in lesions with OCT-defined TCFA-containing intima and OCT-measured fibrous cap was thinner in lesions with VH-IVUS-defined TCFA-containing intima.

Finally, recent clinical studies have suggested that there may be a late catch-up phenomenon in some patients after DES implantation.[36] The current findings suggest that the mechanism of late catch-up may be in-stent neoatherosclerosis and not just progressive IH.

Limitations

First, the present study is not a true study of the natural history of stented lesions in which the same stents are serially studied at different time periods after implantation. Second, the sample size was relatively small, and all patients were symptomatic and presented relatively late because of DES failure. Therefore, we cannot comment on the frequency of these findings in unselected patients after DES placement, especially patients who present with earlier DES failure. Third, we could not demonstrate the impact of these OCT findings on long-term clinical events. Fourth, patients with angiographically visible thrombi with high embolic risk and hemodynamic instability were excluded from OCT imaging. There are differences in drug, release kinetics, and polymers among the different DES. We studied only ISR lesions in which IH was the dominant mechanism of restenosis, excluding stented lesions showing underexpansion with little neointima. Therefore, the current findings cannot be applied to the population with acute myocardial infarction and stent thrombosis or to all types of DES. Fifth, attenuation caused by large amounts of red thrombus obscured underlying neointima morphology; OCT-defined TCFA-containing neointima and neointima rupture were typically seen proximal or distal (or opposite) to the red thrombus and not behind the thrombus, which might have lead to an underestimation of the presence of TCFA-containing neointima and neointimal ruptures. Sixth, the incidence of VH-defined TCFA-containing intima and %NC might be underestimated in lesions with mural thrombi. Seventh, even though VH-IVUS has been applied to clinical research, the accuracy of necrotic core detection using VH-IVUS versus real histology has been debatable among studies of human and porcine coronary lesions.[29,37] Moreover, VH-IVUS characterization of neointima has never been validated. With the lack of histological confirmation, future pathological studies are necessary to validate these OCT and particularly these VH-IVUS findings.

Eighth, we cannot exclude the possibility that the OCT procedure may have contributed to some of the findings such as neointimal rupture; however, patients who required predilation before the OCT imaging were systematically excluded. Finally, many of the OCT neointimal ruptures and thrombi were small, especially in stable patients, and were evidence of in-stent neoatherosclerosis causing ISR and were not responsible for clinical instability.

Conclusion

The current OCT findings demonstrate in-stent TCFA-containing neointima, neointimal rupture, and thrombi in DES failure patients presenting with ISR (whether stable or unstable). These findings suggest that in-stent neoatherosclerosis assessed by OCT and VH-IVUS may be an important mechanism of DES failure, especially late after implantation.

Source of Funding

All of the authors report receiving grant support from the Korea Health 21 R&D Project, Ministry of Health and Welfare, Korea (A090264).

Disclosures

None.

References

1. Kimura T, Yokoi H, Nakagawa Y, Tamura T, Kaburagi S, Sawada Y, Sato Y, Yokoi H, Hamasaki N, Nosaka H, Nobuyoshi M. Three-year follow-up after implantation of metallic coronary-artery stents. *N Engl J Med*. 1996;334:561–566.
2. Schatz RA, Palmaz JC, Tio FO, Garcia F, Garcia O, Reuter SR. Balloon expandable intracoronary stents in the adult dog. *Circulation*. 1987;76:450–457.
3. Komatsu R, Ueda M, Naruko T, Kojima A, Becker AE. Neointimal tissue response at sites of coronary stenting in humans: macroscopic, histological, and immunohistochemical analyses. *Circulation*. 1998;98:224–233.
4. Fineschi M, Gori T, Pierli C, Casini S, Sinicropi G, Buti A, Del Pasqua A, Bravi A. Outcome of percutaneous hybrid coronary revascularization: Bare metal stents jeopardize the benefit of sirolimus-eluting stents in the real world. *Can J Cardiol*. 2005;21:1281–1285.
5. Chen MS, John JM, Chew DP, Lee DS, Ellis SG, Bhatt DL. Bare metal stent restenosis is not a benign clinical entity. *Am Heart J*. 2006;151:1260–1264.
6. Kimura T, Abe K, Shizuta S, Odashiro K, Yoshida Y, Sakai K, Kaitani K, Inoue K, Nakagawa Y, Yokoi H, Iwabuchi M, Hamasaki N, Nosaka H, Nobuyoshi M. Long-term clinical and angiographic follow-up after coronary stent placement in native coronary arteries. *Circulation*. 2002;105:2986–2991.
7. Appleby CE, Bui S, Dzavík V. A calcified neointima: "stent" within a stent. *J Invasive Cardiol*. 2009;21:141–143.
8. Habara M, Terashima M, Suzuki T. Detection of atherosclerotic progression with rupture of degenerated in-stent intima five years after bare-metal stent implantation using optical coherence tomography. *J Invasive Cardiol*. 2009;21:552–553.
9. Hasegawa K, Tamai H, Kyo E, Kosuga K, Ikeguchi S, Hata T, Okada M, Fujita S, Tsuji T, Takeda S, Fukuhara R, Kikuta Y, Motohara S, Ono K, Takeuchi E. Histopathological findings of new in-stent lesions developed beyond five years. *Catheter Cardiovasc Interv*. 2006;68:554–558.
10. Higo T, Ueda Y, Oyabu J, Okada K, Nishio M, Hirata A, Kashiwase K, Ogasawara N, Hirotani S, Kodama K. Atherosclerotic and thrombogenic neointima formed over sirolimus drug-eluting stent: an angioscopic study. *JACC Cardiovasc Imaging*. 2009;2:616–624.
11. Kang SJ, Mintz GS, Park DW, Lee SW, Kim YH, Lee CW, Han KH, Kim JJ, Park SW, Park SJ. Tissue characterization of in-stent neointima using intravascular ultrasound radiofrequency data analysis. *Am J Cardiol*. 2010;106:1561–1565.
12. Takano M, Yamamoto M, Inami S, Murakami D, Ohba T, Seino Y, Mizuno K. Appearance of lipid-laden intima and neovascularization after implantation of bare-metal stents extended late-phase observation by intracoronary optical coherence tomography. *J Am Coll Cardiol*. 2009;55:26–32.
13. Mehran R, Dangas G, Abizaid AS, Mintz GS, Lansky AJ, Satler LF, Pichard AD, Kent KM, Stone GW, Leon MB. Angiographic patterns of in-stent restenosis: classification and implications for long-term outcome. *Circulation*. 1999;100:1872–1878.
14. Ryan TJ, Faxon DP, Gunnar RM, Kennedy JW, King SB III, Loop FD, Peterson KL, Reeves TJ, Williams DO, Winters WL Jr. Guidelines for percutaneous transluminal coronary angioplasty: a report of the American College of Cardiology/American Heart Association Task Force on Assessment of Diagnostic and Therapeutic Cardiovascular Procedures (Subcommittee on Percutaneous Transluminal Coronary Angioplasty). *Circulation*. 1988;78:486–502.
15. Popma JJ, Leon MB, Moses JW, Holmes DR Jr, Cox N, Fitzpatrick M, Douglas J, Lambert C, Mooney M, Yakubov S, Kuntz RE; SIRIUS Investigators. Quantitative assessment of angiographic restenosis after sirolimus-eluting stent implantation in native coronary arteries. *Circulation*. 2004;110:3773–3780.
16. Lee SW, Park SW, Kim YH, Yun SC, Park DW, Lee CW, Hong MK, Rhee KS, Chae JK, Ko JK, Park JH, Lee JH, Choi SW, Jeong JO, Seong IW, Cho YH, Lee NH, Kim JH, Chun KJ, Kim HS, Park SJ. A randomized comparison of sirolimus- versus paclitaxel-eluting stent implantation in patients with diabetes mellitus. *J Am Coll Cardiol*. 2008;52:727–733.
17. Xie Y, Takano M, Murakami D, Yamamoto M, Okamatsu K, Inami S, Seimiya K, Ohba T, Seino Y, Mizuno K. Comparison of neointimal coverage by optical coherence tomography of a sirolimus-eluting stent versus a bare metal stent three months after implantation. *Am J Cardiol*. 2008;102:27–31.
18. Gonzalo N, Garcia-Garcia HM, Regar E, Barlis P, Wentzel J, Onuma Y, Ligthart J, Serruys PW. In vivo assessment of high-risk coronary plaques at bifurcations with combined intravascular ultrasound virtual histology and optical coherence tomography. *JACC Cardiovasc Imaging*. 2009;2:473–482.
19. Yabushita H, Bouma BE, Houser SL, Aretz HT, Jang IK, Schlendorf KH, Kauffman CR, Shishkov M, Kang DH, Halpern EF, Tearney GJ. Characterization of human atherosclerosis by optical coherence tomography. *Circulation*. 2002;106:1640–1645.
20. Regar E, van Beusekom HMM, van der Gissen WJ, Serruys PW. Optical coherence tomography findings at 5-year follow-up after coronary stent implantation. *Circulation*. 2005;112:e345–e346.
21. Prati F, Regar E, Mintz GS, Arbustini E, Di Mario C, Jang IK, Akasaka T, Costa M, Guagliumi G, Grube E, Ozaki Y, Pinto F, Serruys PW; Expert's OCT Review Document. Expert review document on methodology, terminology, and clinical applications of optical coherence tomography: physical principles, methodology of image acquisition, and clinical application for assessment of coronary arteries and atherosclerosis. *Eur Heart J*. 2010;31:401–415.
22. Kume T, Akasaka T, Kawamoto T, Ogasawara Y, Watanabe N, Toyota E, Neishi Y, Sukmawan R, Sadahira Y, Yoshida K. Assessment of coronary arterial thrombus by optical coherence tomography. *Am J Cardiol*. 2006;97:1713–1717.
23. Jang IK, Tearney GJ, MacNeill, Takano M, Moselewski F, Iftima N, Shishkov M, Houser S, Aretz HT, Halpern EF, Bouma BE. In vivo characterization of coronary atherosclerotic plaque by use of optical coherence tomography. *Circulation*. 2005;111:1551–1555.
24. Gonzalo N, Serruys PW, Okamura T, van Beusekom HM, Garcia-Garcia HM, van Soest G, van der Giessen W, Regar E. Optical coherence tomography patterns of stent restenosis. *Am Heart J*. 2009;158:284–293.
25. Park SJ, Shim WH, Ho DS, Raizner AE, Park SW, Hong MK, Lee CW, Choi D, Jang Y, Lam R, Weissman NJ, Mintz GS. A paclitaxel-eluting stent for the prevention of coronary restenosis. *N Engl J Med*. 2003;348:1537–1545.
26. Mintz GS, Weissman NJ, Teirstein PS, Ellis SG, Waksman R, Russo RJ, Moussa I, Tripuraneni P, Jani S, Kobayashi Y, Giorgianni JA, Pappas C, Kuntz RA, Moses J, Leon MB. Effect of intracoronary gamma-radiation therapy on in-stent restenosis: An intravascular ultrasound analysis from the gamma-1 study. *Circulation*. 2000;102:2915–2918.
27. Finn AV, Nakazawa G, Joner M, Kolodgie FD, Mont EK, Gold HK, Virmani R. Vascular responses to drug eluting stents: importance of delayed healing. *Arterioscler Thromb Vasc Biol*. 2007;27:1500–1510.
28. Sonoda S, Morino Y, Ako J, Terashima M, Hassan AH, Bonneau HN, Leon MB, Moses JW, Yock PG, Honda Y, Kuntz RE, Fitzgerald PJ; SIRIUS Investigators. Impact of final stent dimensions on long-term results following sirolimus-eluting stent implantation: serial intravascular

ultrasound analysis from the SIRIUS trial. *J Am Coll Cardiol.* 2004;43:1959–1963.
29. Nair A. Kuban BD, Tuzcu EM, Schoenhagen P, Nissen SE, Vince G. Coronary plaque classification with intravascular ultrasound radiofrequency data analysis. *Circulation*. 2002;106:2200–2206.
30. Rodriguez-Granillo GA, García-García HM, Mc Fadden EP, Valgimigli M, Aoki J, de Feyter P, Serruys PW. In vivo intravascular ultrasound-derived thin-cap fibroatheroma detection using ultrasound. *J Am Coll Cardiol.* 2005;46:2038–2042.
31. Guagliumi G, Sirbu V. Optical coherence tomography: high resolution intravascular imaging to evaluate vascular healing after coronary stenting. *Catheter Cardiovasc Interv.* 2008;72:237–247.
32. Nakazawa G, Vorpahl M, Finn AV, Narula J, Virmani R. One step forward and two steps back with drug-eluting-stents: from preventing restenosis to causing late thrombosis and nouveau atherosclerosis. *JACC Cardiovasc Imaging*. 2009;2:625–628.
33. Lee CW, Kang SJ, Park DW, Lee SH, Kim YH, Kim JJ, S Park SW, Mintz GS, Park SJ. Intravascular ultrasound findings in patients with very late stent thrombosis after either drug-eluting or bare-metal stent implantation. *J Am Coll Cardiol*. 2010;55:1936–1942.
34. Kubo T, Imanishi T, Takarada S, Kuroi A, Ueno S, Yamano T, Tanimoto T, Matsuo Y, Masho T, Kitabata H, Tsuda K, Tomobuchi Y, Akasaka T. Assessment of culprit lesion morphology in acute myocardial infarction: ability of optical coherence tomography compared with intravascular ultrasound and coronary angioscopy. *J Am Coll Cardiol*. 2007;50:933–939.
35. Sawada T, Shite J, Garcia-Garcia HM, Shinke T, Watanabe S, Otake H, Matsumoto D, Tanino Y, Ogasawara D, Kawamori H, Kato H, Miyoshi N, Yokoyama M, Serruys PW, Hirata K. Feasibility of combined use of intravascular ultrasound radiofrequency data analysis and optical coherence tomography for detecting thin-cap fibroatheroma. *Eur Heart J*. 2008;29:1136–1146.
36. Stettler C, Wandel S, Allemann S, Kastrati A, Morice MC, Schömig A, Pfisterer ME, Stone GW, Leon MB, de Lezo JS, Goy JJ, Park SJ, Sabaté M, Suttorp MJ, Kelbaek H, Spaulding C, Menichelli M, Vermeersch P, Dirksen MT, Cervinka P, Petronio AS, Nordmann AJ, Diem P, Meier B, Zwahlen M, Reichenbach S, Trelle S, Windecker S, Jüni P. Outcomes associated with drug-eluting and bare-metal stents: a collaborative network meta-analysis. *Lancet*. 2007;370:937–948.
37. Thim T, Hagensen MK, Wallace-Bradley D, Granada JF, Kaluza GL, Drouet L, Paaske WP, Bøtker HE, Falk E. Unreliable assessment of necrotic core by virtual histology intravascular ultrasound in porcine coronary artery disease. *Circ Cardiovasc Imaging*. 2010;3:384–391.

CLINICAL PERSPECTIVE

We report the findings from optical coherence tomography (OCT) of in-stent neoatherosclerosis as a cause of drug-eluting stent failure. Optical coherence tomography was performed in a total of 50 lesions with angiographic in-stent restenosis (30 stable and 20 unstable angina). Optical coherence tomography–defined thin-cap fibroatheroma (TCFA)–containing neointima, thrombi, and neointimal rupture were identified in lesions with significant intimal hyperplasia (>50% of stent area). Median follow-up time was 32 months. Overall, 26 lesions (52%) had in-stent TCFA-containing neointima, and 29 (58%) had neointimal rupture. Patients presenting with unstable angina showed a thinner fibrous cap (55 μm [interquartile range 42 to 105] versus 100 μm [interquartile range 60 to 205], $P=0.006$) and higher incidence of TCFA-containing neointima (75% versus 37%, $P=0.008$), intimal rupture (75% versus 47%, $P=0.044$), thrombi (80% versus 43%, $P=0.010$), and red thrombi (30% versus 3%, $P=0.012$) than those presenting with stable angina. Fibrous cap thickness negatively correlated with follow-up time ($r=-0.318$, $P=0.024$). Compared with stent <20 months after implantation (the best cut-off to predict TCFA-containing neointima), stent ≥20 months after implantation had a higher incidence of TCFA-containing neointima (69% versus 33%, $P=0.012$) and red thrombi (27% versus 0%, $P=0.007$). Postintervention creatine kinase MB was significantly higher in intimal rupture versus no intimal rupture ($P=0.025$). The rate of agreement between grayscale intravascular ultrasound and OCT for detecting intimal rupture was 50% and for detecting thrombus was 44%. In the virtual histology intravascular ultrasound subgroup (N=32), the agreement between virtual histology intravascular ultrasound and OCT for identifying TCFA-containing neointima was 78%. Thus, in-stent neoatherosclerosis may be an important mechanism of drug-eluting stent failure especially late after implantation.

SUPPLEMENTAL MATERIAL

; supplemental results and Tables from VH subgroup analysis in 32 lesions

Baseline clinical and procedural characteristics. The clinical and procedural characteristics of the 32 DES-ISR patients who had imaging using all three modalities (grayscale and VH-IVUS and OCT) were summarized in supplemental Table 1. The median follow-up time in 32 patients (20 stable and 12 unstable angina) was 17.2 months (IQR 8.9 ï 50.8 months). At the time of follow-up angiography, 20 (63%) patients presented with stable angina and 12 (37%) patients with unstable angina.

Angiographic and IVUS findings. Quantitative angiographic and grayscale IVUS data in 32 patients were presented in supplemental Table 2. At the MLA site using IVUS, 5 stents (16%) were underexpanded (minimal stent area <5.0mm^2). Also using grayscale IVUS, in-stent neointimal ruptures were detected in 3 lesions (9%) and thrombi were detected in 4 lesions (13%).

VH-IVUS findings. Overall, 13 (41%) ISR lesions showed NC >10% at the MLA site; and 24 (75%) had NC >10% at the maximal NC site. Compared to lesions with Ò10% NC at the MLA site, lesions with >10% NC had significantly longer time to ISR presentation (46.3 months [14.7 ï 63.3 months] vs. 10.2 months [7.7 ï 43.7 months], p=0.040).

VH-defined TCFA-containing neointima was seen in 10 (31%) lesions. The 10 lesions with a TCFA-containing neointima presented later than the 22 lesions without a TCFA-containing neointima: 49.2 months (IQR 15.9 ï 66.8 months) vs. 11.6 months (IQR 7.7 ï 41.6 months), (p=0.006). Also, there was a positive correlation between follow-up time and %DC at the maximal %NC site (r=0.510, p=0.015). The axial distribution of the TCFA-containing neointima was at the MLA site in 50%, proximal to the MLA site in 29%, and distal to the MLA site in 21%. In supplemental Table 3, VH-IVUS characteristics are compared according to the clinical presentation of ISR

OCT findings. Overall, 15 (47%) lesions had at least one site of in-stent TCFA-containing neointima; and 19 (59%) had at least one site of in-stent neointimal rupture. The axial location of neointimal ruptures was at the MLA site in 46%, proximal to the MLA site in 46%, and distal to the MLA site in 8%. In addition, the axial location of the TCFA-containing neointima was at the MLA site in 45%, proximal to the MLA site in 33%, and distal to the MLA site in 22%. Thrombi were identified in 27 (68%) patients. In supplemental Table 4, OCT characteristics are compared according to the clinical presentation of ISR (unstable angina vs. stable angina). OCT-measured fibrous cap thickness negatively correlated with time to presentation (r=-0.339, p=0.048).

ıe clinical and procedural characteristics in 32 patients

Variable	
Baseline clinical characteristics	
Age (years)	62 (54 ï 68)
Male, N (%)	26 (81%)
Smoking, N (%)	17 (53%)
Hypertension, N (%)	17 (53%)
Hypercholesterolemia, N (%)	26 (81%)
Diabetes mellitus, N (%)	11 (34%)
Left ventricular ejection fraction, %	60 (57 ï 63)
Previous coronary bypass surgery, N (%)	0 (0%)
Previous myocardial infarction, N (%)	1 (3%)
Types of drug-eluting stent	
Cypher, N (%)	17 (53%)
Taxus, N (%)	5 (16%)
Xience, N (%)	2 (6%)
Other drug-eluting stent, N (%)	8 (25%)
Total stent length, mm	30 (23 ï 46)

Median value (inter-quartile range)

raphic and intravascular ultrasound data in 32 lesions

Variable	
Angiographic findings	
Lesion location, N (%)	
Left anterior descending, N (%)	20 (62%)
Left circumflex, N (%)	2 (6%)
Right coronary. N (%)	10 (32%)
Proximal reference diameter, mm	3.2 (2.9 ï 3.6)
Distal reference diameter, mm	2.6 (2.1 ï 3.0)
Minimal lumen diameter, mm	0.9 (0.5 ï 1.1)
Diameter stenosis,%	71.0 (60.0 ï 81.8)
TIMI flow	
TIMI 0, N (%),	2 (6%)
TIMI 1, N (%)	1 (3%)
TIMI 2, N (%)	4 (13%)
TIMI 3, N (%)	25 (78%)
Stent fracture, N (%)	3 (9%)
Mehran Classification	
Focal in-stent restenosis, N (%)	8 (25%)
Multifocal in-stent restenosis, N (%)	13 (41%)
Diffuse in-stent restenosis, N (%)	10 (31%)
Total in-stent restenosis, N (%)	1 (3%)
Intravascular ultrasound findings	
Proximal reference lumen area, mm^2	6.8 (5.4 ï 8.1)

ım^2	15.5 (11.4 ï 17.8)
Distal reference lumen area, mm^2	4.5 (3.5 ï 5.7)
Distal reference EEM area, mm^2	7.9 (6.2 ï 11.3)
Minimal stent area, mm^2	5.8 (4.8 ï 7.4)
Minimal lumen area, mm^2	1.9 (1.2 ï 2.6)
Stent area at the minimal lumen site, mm^2	6.8 (5.5 ï 8.2)
IH, %	70.7 (62.8 ï 77.8)

TIMI, Thrombolysis In Myocardial Infarction

Median value (inter-quartile range)

Supplemental Table 3. VH findings according to clinical presentation

	Total	Stable	Unstable	P value
N	32	20	12	
At the MLA site				
Fibrous, %	71.6 (63.8 ï 78.7)	73.7 (60.3 ï 80.8)	71.6 (66.5 ï 75.4)	0.578
Fibrofatty,%	13.5 (3.7 ï 23.3)	12.7 (4.1 ï 30.7)	18.9 (3.7 ï 23.3)	0.716
Necrotic core, %	8.3 (1.8 ï 23.3)	8.3 (1.7 ï 17.4)	9.8 (1.9 ï 23.1)	0.687
Dense calcium, %	0.8 (0.0 ï 2.0)	0.8 (0.0 ï 2.1)	0.9 (0.0 ï 1.8)	0.954
Incidence of %NC >10%	13 (41%)	7 (35%)	6 (50%)	0.320
At the maximal necrotic core site				
Fibrous, %	66.7 (56.6 ï 75.2)	71.6 (53.3 ï 75.7)	64.9 (60.4 ï 73.6)	0.687
Fibrofatty,%	4.0 (1.9 ï 15.2)	3.8 (0.8 ï 12.3)	3.9 (2.9 ï 20.8)	0.501
Necrotic core, %	20.7 (9.1 ï 31.3)	21.0 (7.1 ï 33.1)	22.8 (12.1 ï 31.2)	0.803
Dense calcium, %	1.5 (0.2 ï 5.1)	1.2 (0.2 ï 5.6)	1.7 (1.1 ï 3.8)	0.985
Incidence of %NC >10%	24 (75%)	14 (70%)	10 (83%)	0.344

Continuous variables are presented as median value (inter-quartile range) and compared using non-parametric, Mann-Whitney test

Supplemental Table 4. OCT findings according to clinical presentation in 32 lesions

	Total	Clinical presentation		
		Stable	Unstable	P value
N	32	20	12	
Lipid neointima, N (%)	29 (91%)	17 (85%)	12 (100%)	0.230
Min. thickness of fibrous cap, μm	60.0 (50.0 ï 180.0)	100.0 (52.5 ï 215.0)	50.0 (40.0 ï 120.0)	0.016
Incidence of thrombi, N (%)	20 (63%)	10 (50%)	10 (83%)	0.059
Incidence of intimal rupture, N (%)	19 (59%)	12 (60%)	7 (58%)	0.926
Incidence of multiple ruptures, N (%)	5 (16%)	2 (10%)	3 (25%)	0.258
Incidence of TCFA, N (%)	15 (47%)	8 (38%)	14 (74%)	0.024
Incidence of multiple TCFA, N (%)	4 (13%)	2 (10%)	2 (17%)	0.581

Continuous variables are presented as median value (inter-quartile range) and compared using non-parametric, Mann-Whitney test